Journal of Materials and Environmental Sciences
ISSN : 2028-2508
CODEN : JMESCN

J. Mater. Environ. Sci., 2019, Volume 10, Issue 1, Page 22-31

http://www.jmaterenvironsci.com

Aqueous extract of *Dillenia Pentagyna* Fruit as green inhibitor for mild steel corrosion in 0.5 M hydrochloric acid solution

Manjunath Hegde[1*], S. P. Nayak[2]

[1*]*Department of Chemistry, S.D.M. College, Honavar, Karnataka 581334, India*
[2]*Department of Chemistry, Mangalore University, Mangalagangotri, Karnataka 574199, India*

Received 17 March 2019,
Revised 14 April 2019,
Accepted 12 April 2019

Keywords
✓ *Dillenia pentagyna* Fruit,
✓ Mild steel,
✓ Adsorption,
✓ Tafel Plot.

kmanjuhegde@gmail.com
Phone: +919480789522

Abstract

An aqueous extract of *Dillenia pentagyna* Fruits (DPF) was studied as corrosion inhibitor on mild steel in 0.5 M hydrochloric acid using conventional weight loss method and electrochemical methods. The increase of corrosion rate on mild steel is influenced by the increase of temperature and decrease of DPF concentration. The efficiency of Corrosion Inhibition increases with increase of extract concentration. The adsorption of DPF extract on mild steel surface is associated with Langmuir adsorption isotherm. Electrochemical measurement shows that DPF extract behaves as mixed type inhibitor. The protective nature of DPF extract on mild steel film is reflected by Scanning electron microscope images.

1. Introduction

Mild steel is the most common constructive material in chemical and allied industries because of its good strength, hardness, and easy availability in very cheap rate. In chemical industry, hydrochloric acid is mainly used in the manufacture, processing, storage, or transportation, which creates aggressive environment [1]. The mild steel is exposed to aggressive environment under atmospheric condition and the metal becomes corroded. The control of corrosion oil or grease is used as coating materials. But it is not significant due to high labor, material cost for the application. The corrosion inhibitors which are simple, cheap and have strong adsorption characteristics are used to control the degradation of metals. At presently synthesized organic compounds are used as corrosion inhibitors. But the root of synthesis is more expensive and toxic in nature. To reduce the cost and toxic nature, renewable sources of materials are introduced, which are naturally occurring antioxidants, easily available and cheap materials [2].

The green inhibitors are easily biodegradable due to their biological origin. The polar atoms contain lone pair of electrons such as S, N, O, P are adsorbed on metal surface and creates protective film. It blocks the surface of the metal at very low concentration and protects the metal from corrosion [3,4]. To resolve this problem of corrosion large amount of emulsions, and inhibiters are utilized, but these substances are harmful and non-ecofrendly. Therefore; in this present study we are trying to develop natural substances which are capable to substitute these harmful substances and with good efficiency against the corrosion inhibition similar to the non ecofriendly substance.

Dillenia pentagyna is a large deciduous evergreen tree available in coastal area of the Uttara Kannada located in Karnataka and having pharmacological activities like Antitumour, antimicrobial, anticancer, anti-alpha glucosidase, antioxidant, antidiabetic, antifungal, antidiarrheal, cytotoxic and lymphocytic activities [5-8]. Literature study reveals that the *Dillenia pentagyna* is a rich source of quercetin, betulin, betulinic acid, β-sitosterol, dipoloic acid and myricetin [9-11], its chemical structures are illustrated in Figure 1. These flavanoid derivatives protect the metal surfaces as corrosion inhibitors in acidic environment. There are no reports on use of *Dillenia pentagyna* fruit extract as corrosion inhibitor for mild steel in HCl solution. Hence in the present study the aqueous extraction of DP fruit is used as anticorrosive property on mild steel in 0.5 M HCl solution using mass loss and electrochemical methods. Protected surface of the mild steel was studied by scanning electron microscopy (SEM).

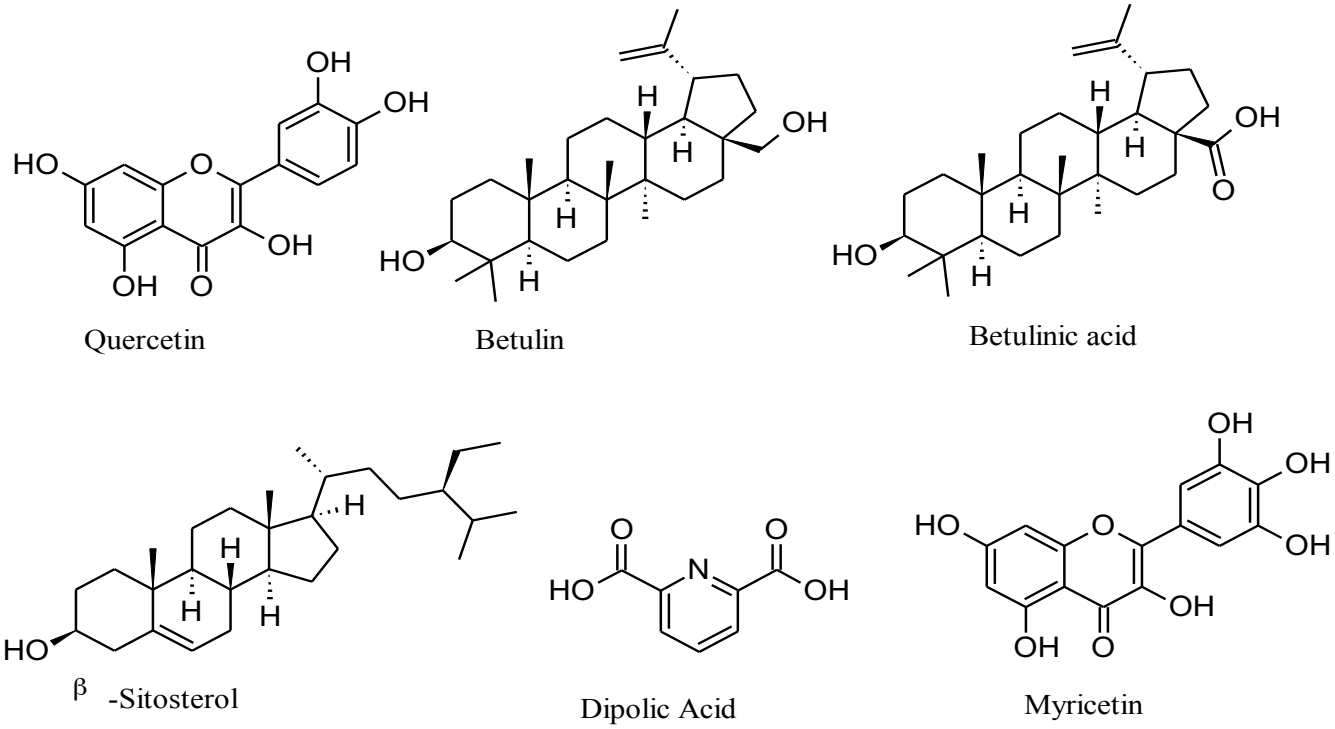

Figure 1: Chemical compositions of DPF extract

2. Materials and Methods

2.1. Materials

The sheet of mild steel having the chemical composition: 0.16% Carbon, 0.032% Manganese, 0.18% Silicon, 0.026% Sulphur, 0.03% Phosphorous and remaining of Iron cut into coupon of size 2.6 cm x 2 cm x 0.025 cm is used for mass loss as well as electrochemical studies. The surface of the mild steel coupon was cleaned by polishing with emery paper, washing the coupon with acetone and double distilled water to remove the dust and impurities on the surface before using in each measurements.

2.2. Extraction of Dillenia pentagyna fruit

A domestic microwave oven (KOG- 3767, DAEWOO), used in this study, had a total capacity of 850 W8. Seed samples (5 g) were mixed with the distilled water (100 ml) in 250 ml conical flask. The resulting mixtures were irradiated in microwave oven at the interval of 10 minutes. The warm extractant was filtered quickly through a Whatman filter paper No. 41 and filtrates were collected in a clean dry petri dish and concentrated using an incubator maintained at 40º C for about 10 hr. Inhibitor was prepared in the concentration range of 0.2– 0.8 g/L.

2.3. FT-IR Spectral Studies of DPF extract

Prestige-21 FT-IR spectrophotometer was used to identify the functional group present in DPF extract with the wave number range from 4000 to 400 cm^{-1}.

2.4. Mass loss methods

The gravimetric study is the easiest method to determine the corrosion rate and inhibition efficiency of the inhibitor by dipping the previously weighed mild steel coupon in 100ml solution containing different concentration of the DPF extract for the period of 1 hour and the temperature maintained at 30 ^{0}C to 50 ^{0}C using thermostat. After one hour the coupon was remove and washed with double distilled water, dried and reweighed. The loss of weight due to corrosion of mild steel was noted. The experiment was repeated in triplicate with 0.5M HCl as blank.

From the mass loss values, rate of corrosion (C_R) at different concentrations of inhibitor was calculated [12] by the equation,

$$C_{R\,(mmpy)} = \frac{87.6 \times W}{Atd} \qquad (1)$$

Where weight loss W (mg), surface area of coupon A (cm^2), immersion time t (h), and density of mild steel d (7.85 g cm^{-3}).
The inhibition efficiency (η %) and surface coverage (θ) of the DPF extract were evaluated from the following formulae,

$$\eta\ (\%) = \frac{(W1 - W2)}{W1} \times 100 \qquad (2)$$

$$\Theta = \frac{(W1 - W2)}{W1} \qquad (3)$$

Where, W_2 and W_1 are the weight loss of the mild steel in the presence and absence of the DPF extract respectively in 0.5 M HCl at the same temperature.

2.5. Electrochemical Methods

All electrochemical experiments were performed in a one-compartment cell at 30° C where working electrode is mild steel coupon, counter electrode is platinum wire and reference electrode is saturated calomel electrode. These three electrodes are connected to Electrochemical Workstation, CHI6O4E (CH instruments).
The mild steel coupon was connected in the direction of potential from cathodic to anodic side in potentiodynamic polarization (Tafel) measurements. Tafel curves were recorded by changing the electrode potential from cathodically -200 mV to anodically +200 mV at a scan rate of 0.01 V/s.
AC impedance measurements were recorded by adjusting the amplitude of 0.01 V of AC signal at OCP over a frequency range of 1mHz – 100 kHz with 5 mV amplitude.

2.6. Surface Morphology

The surface morphological study was done by scanning electron microscopy CARL ZEISS FESEM instrument at high vacuum and the accelerating voltage of 5 kV. The precleaned mild steel coupons were immersed in blank solution 0.5 M HCl and 0.8g/L of DPF extract solution for a period of 5 hours at 30°C and submitted the dried coupons for SEM analysis.

3. Results and Discussion

3.1. Mass loss measurements

The mild steel corroded faster in pure 0.5 M HCl solution than in acid containing DPF extract solution. The different concentration like 0.3, 0.6, 0.9 and 1.2 g/L of DPF extract in 0.5 M HCl solution changing the corrosion rate of mild steel was studied by weight loss method. This method explains the decrease in the rate of corrosion with increase in DPF extract concentration and inhibition efficiency increases with increase in DPF extract concentration up to 1.2 g/L in acid solution. Above this concentration, there is no drastic change in the inhibition efficiency value. The corrosion rate and inhibition efficiency changes with concentration are reported in Table 1. The result shows inhibition efficiency of DPF extract maximum up to 92.29 % at 1.2 g/L concentration.

3.1.1. Effect of temperature

The rate of corrosion varies with temperature and activation parameters were calculated by change in temperature from 303 K to 323 K for different concentration of DPF extract. From the Table 1, it is clear that the corrosion rate increases with increasing temperature and the inhibition efficiency of different concentrations of DPF extract decreases due to increase in the solubility of protective film at higher temperature. The variations of corrosion rate and inhibition efficiency with different concentration of the extract at all temperature are shown in the Figure 2 and Figure 3 respectively.

The dependence of corrosion rate on varied temperature, the activation parameters such as activation energy (E_a), enthalpy (ΔH^*) and entropy (ΔS^*) of corrosion process were computed with the help of Arrhenius equation and transition-state equation respectively [13,14]

$$\ln C_R = \ln A - \frac{E_a}{RT} \qquad (4)$$

$$\ln \frac{C_R}{T} = \left[\ln \frac{R}{Nh} + \frac{\Delta S^*}{R}\right] - \frac{\Delta H^*}{RT} \qquad (5)$$

Where C_R is the corrosion rate, A is the Arrhenius pre-exponential factor T is the absolute temperature, R is the universal gas constant, N is Avogadro's number and h is Planck's constant.

Table 1: Corrosion rate and Inhibition efficiency varied with concentration at variable temperature.

Temperature (K)	Concentration g/L	Corrosion rate(mmpy)	Inhibitor Efficiency IE (%)	Degree of surface coverage θ
303	Blank	39.47	-	-
	0.3	12.60	68.09	0.6809
	0.6	9.55	75.80	0.7580
	0.9	6.51	83.51	0.8351
	1.2	3.04	92.29	0.9229
308	Blank	43.15	-	-
	0.3	16.38	62.04	0.6204
	0.6	11.34	73.72	0.7372
	0.9	7.77	82.00	0.8200
	1.2	4.30	90.02	0.9002
313	Blank	47.35	-	-
	0.3	19.32	59.20	0.5920
	0.6	13.75	70.95	0.7095
	0.9	9.47	80.00	0.8000
	1.2	5.67	88.03	0.8803
318	Blank	52.70	-	-
	0.3	22.68	56.97	0.5697
	0.6	16.90	67.93	0.6793
	0.9	12.07	77.09	0.7709
	1.2	7.87	85.06	0.8506
323	Blank	57.21	-	-
	0.3	25.72	55.05	0.5505
	0.6	19.42	66.06	0.6606
	0.9	14.28	75.05	0.7506
	1.2	9.76	82.94	0.8294

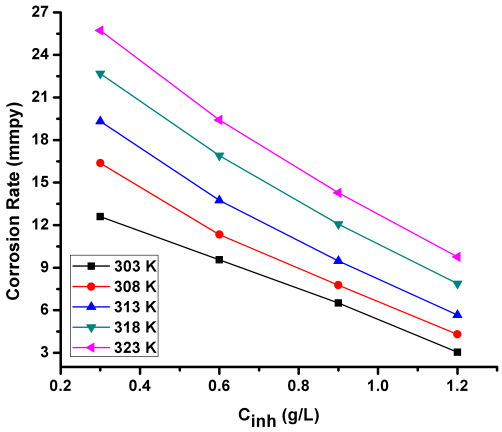

Figure 2: corrosion rate varies with temperature

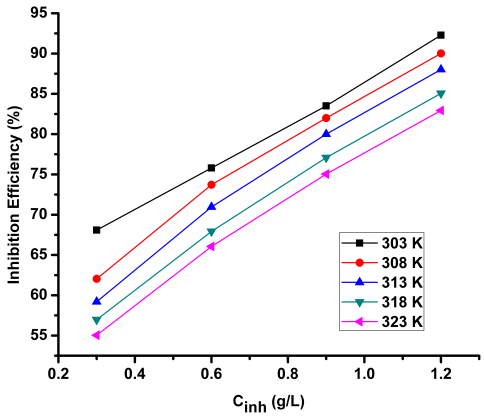

Figure 3: Inhibition efficiency increases with concentration

Figure 4 expresses the Arrhenius plot *ln CR vs. 1/T* with straight lines having the slope $-Ea^*/R$ and intercept ln A. Figure 5 shows the transition state plot $\ln(C_R/T)$ vs. 1/T, the slope $(-\Delta H^*/R)$ and an intercept of $[\ln(R/Nh)) + (\Delta S^*/R)]$ obtained from straight lines. From these plots calculated activation parameters are listed in Table 2. It

was observed that, E_a^* value is 15.33 kJ/mol in pure HCl solution and it changes from 28.59 to 47.80 kJ/mol in 0.3 to 1.2 g/L concentration of the inhibitor respectively. The increases in the activation energy clarify the physical adsorption on the mild steel surface.

Table 2: Activation parameters

Concentration (g/L)	E_a^* (kJ/mol)	A (kJ/mol)	ΔH^* (kJ/mol)	ΔS^* (J/mol/K)
Blank	15.33	17.27×10^3	12.73	-172.51
0.3	28.59	11.16×10^5	25.99	-137.85
0.6	29.60	12.02×10^5	27.00	-137.24
0.9	32.73	28.05×10^5	30.13	-130.19
1.2	47.80	54.04×10^7	45.20	-86.45

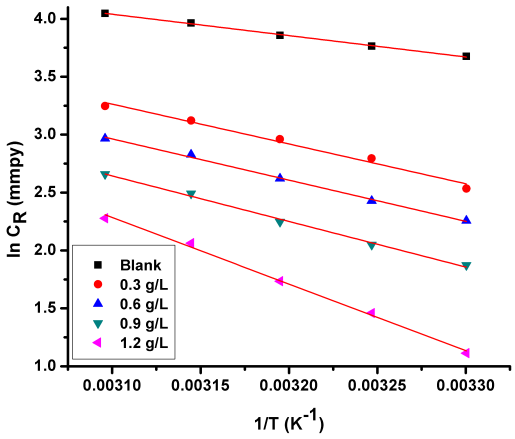

Figure 4: Arrhenius plot in different concentration of inhibitor

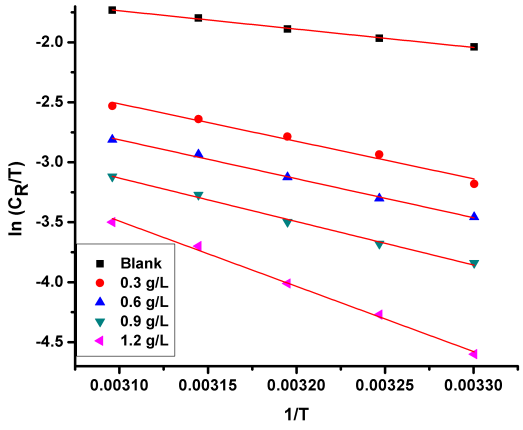

Figure 5: Transition-state plot

The increase of the positive values of ΔH^* from zero concentration to 1.2 g/L of inhibitor concentration reveals that the control of metal dissolution is endothermic in nature. That the E_a^* values are always greater than ΔH^* indicates the corrosion of the metal involved in gaseous reaction. The negative values of ΔS^* confirms the decrease in disorderliness. The reaction moves from reactants to activated complex and the association of activated complex is the rate determining step [15].

The adhesion of dissolved solid DPF extracted molecules on the surface of mild steel creates a film on the surface of the adsorbent and protect the metal from the corrosion was elaborated by adsorption isotherm. The behavior of the adsorption is dependent on the amount of surface coverage (θ), were obtained by gravimetric studies. The correlation coefficient (R^2) value decides the suitable adsorption isotherm. The experimental data applied to different adsorption isotherm but R^2 is nearly equal to one from the plot C_{inh} *v/s* C_{inh}/Θ (Figure 6) indicates adsorption behavior obeys Langmuir adsorption isotherm [16] mathematically represented as

$$\frac{C}{\theta} = \frac{1}{K_{ads}} + C \qquad (6)$$

Where, C = Inhibitor concentration, K_{ads} = equilibrium constant

K_{ads} values are calculated for different temperatures and is used for calculation of free energy of adsorption (ΔG^0_{ads}) [17] with the equation,

$$\Delta G^0_{ads} = -2.303RT\log\left(K_{ads}\, C_{H_2O}\right) \qquad (7)$$

Where, C_{H_2O} = water concentration in solution = 1000 g/L

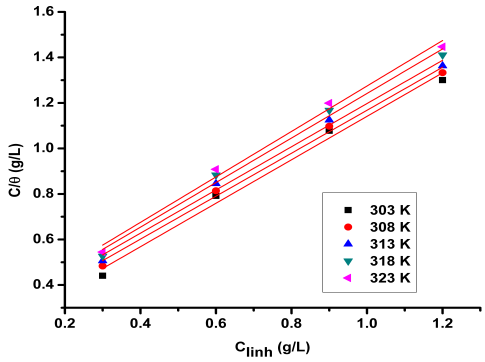

Figure 6: Langmuir adsorption isotherm plot with increase of temperature

The calculated parameters are listed in Table 3. The obtained results indicates that the adsorption process is spontaneous and both at physical and chemical adsorption take place, because ΔG^0_{ads} values are negative and up to -20KJ/mol or lower explains that the transfer of charge between DPF extract molecules to the mild steel surface affects the physical adsorption and ΔG^0_{ads} values more negative than -40KJ/mol show transfer of charge between DPF extract molecules to the mild steel surface affects the chemical adsorption [18-20]. In this investigation average ΔG^0_{ads} values (-39.69 KJ/mol) stretched out between the above limits.

Table 3: Thermodynamic parameters obtained from Langmuir adsorption isotherm.

Temperature (K)	K_{ads} (L/mol)	ΔG^0_{ads} (kJ/mol)
303	5368.55	-39.04
308	4464.88	-39.21
313	4033.23	-39.58
318	3804.74	-40.06
323	3626.87	-40.56

3.2. Electrochemical Measurements

3.2.1. Tafel Plot Studies

Weight loss methods require more time to complete the anticorrosive study. To reduce the time consumption, the polarization methods are adopted. It is the better technique to analyze the corrosion behavior of the metal surfaces. Tafel plot Potential, *E* Vs *log I*, were recorded (Figure 8) when mild steel was dipped in 0.5 M HCl solution and 0.3 g/L to 1.2g/L concentration of DPF extract solutions. Through CH instrument software, corrosion potential E_{corr}, Corrosion current density I_{corr}, cathodic (β_c), and anodic (β_a) Tafel slope were generated. These values helped to determine the Polarization resistance (R_p) on the basis of Stern–Geary equation and the percentage inhibition efficiency (η_p) was calculated [21].

$$R_p = \frac{\beta_a \times \beta_c}{2.303 \times (\beta_a + \beta_c) \times I_{corr}} \qquad (8)$$

$$\eta_p = \left[1 - \frac{I^0_{corr}}{I_{corr}}\right] x\ 100 \qquad (9)$$

I^0_{corr} = corrosion current density in presence of DPF extract and I_{corr}= corrosion current density in 0.5M HCl solution.

The generated $E_{corr,}$ $I_{corr,}$ $\beta_{c,}$ β_a and calculated R_p *and* η_p values are displayed in Table 4. It is noticed from the table, that I_{corr} values decrease from blank solution (0.5M HCl) to 1.2 g/L concentration of the inhibitor and R_p values increase as inhibitor concentration increases. It reveals that, during the adsorption mass and charge of the DPF extracted molecules are transferred to metal surfaces and create protected film on the metal. The efficient inhibitive property of extracted molecules confirmed by η_p values increased to 93.01% at 1.2 g/L of the inhibitor concentration validates the effectual inhibitor.

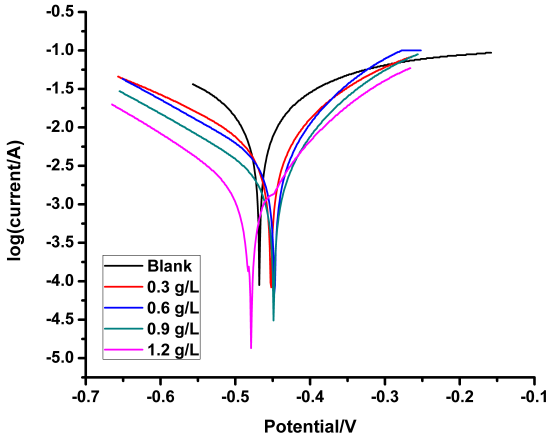

Figure 8: Tafel plot with various concentrations

Table 4: Polarization parameters for mild steel

Concentration (g/L)	E_{corr} (mV)	I_{corr} x 10^{-3} (A)	β_c (V/dec)	β_a (V/dec)	R_p (Ω)	η_p (%)
Blank	-468.1	18.1	5.579	4.71	61.4	-
0.3	-452.1	6.50	5.428	7.100	205	64.01
0.6	-447.3	4.78	5.576	8.684	309	73.57
0.9	-448.3	2.90	5.874	8.903	531	83.97
1.2	-479.0	1.26	6.699	9.980	1380	93.01

If the change in E_{corr} value either <85 mV or >85 mV stands for mixed type inhibitor or inhibitor behaves as anodic/cathodic type respectively. In the present study, the maximum changes in E_{corr} value is 16 mV describes the DPF extract molecule behaves as mixed type. It means anodic and cathodic reactions not varied due to active metal sites are blocked [18].

3.2.2. Electrochemical Impedance Spectroscopic Studies

The corrosion behavior of mild steel in 0.5M HCl solution and inhibition property of the DPF extract at room temperature was investigated by Electrochemical Impedance Spectroscopy (EIS). This study provides information on both the resistive behavior and capacitive behavior at the mild steel metal-solution interface. The impedance data are represented as Nyquist plots recorded in absence and presence of DPF extract are shown in Figure 9.

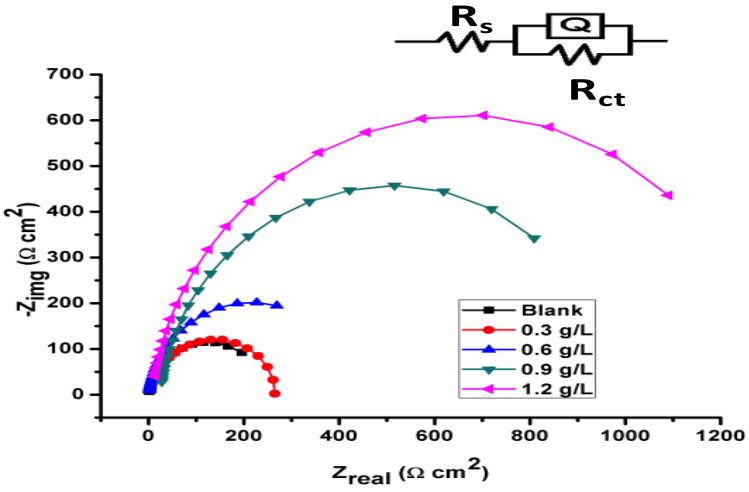

Figure 9: Nyquist Plots

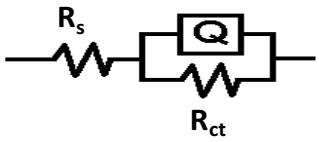

Figure 10: Electrochemical equivalent Circuit of R(QR) model

The data acquisition and analysis of Nyquist curves by using ZSimpWin 3.21 software gives electrical equivalent circuit information represented in Figure 10. From the circuit R_s means the solution resistance, R_{ct} means the charge transfer resistance and Q means the constant phase element (CPE). The CPE used as a capacitor to balance the ideal behavior. The impedance (Z) of CPE was calculated as follows: [22]

$$Z_{CPE} = Q^{-1}(j\omega)^{-n}$$

Where, Q = CPE constant, ω = angular frequency, j = imaginary number, n = CPE exponent.

The values of R_{ct}, Q and n obtained from the circuit helps to calculate double layer capacitance (C_{dl}), and inhibition efficiency η_z from following equations.

$$C_{dl} = (QR_{ct}{}^{1-n})^{1/n}$$

$$\eta_z(\%) = \frac{R_{ct} - R_{ct}^o}{R_{ct}} \times 100$$

Where, R_{ct}^o and R_{ct} are the charge transfer resistances in absence and presence of DPF extract respectively.

The obtained R_{ct}, Q, n and calculated C_{dl}, η_z values are listed in Table 5. The Nyquist curve shows semicircle with high frequency because of charge transfer during the corrosion. The semicircle diameter increases with increasing DPF concentration. The C_{dl} and Q values from the Table 4 decreases as inhibitor concentration increases because of local dielectric constant decreases and electrical double layer thickness increases [23]. The increase of adsorption processes was explained by increase of R_{ct} values. The increase of inhibitor concentration protects the mild steel surfaces by adsorption and charge transfer process increases. This result indicates increase in the inhibition efficiency.

Table 5: Electrochemical Impedance data

Concentration (g/L)	R_{ct} (Ω cm^2)	Q ($\mu\Omega^{-1}S^n cm^{-2}$)	n	C_{dl} (μFcm^{-2})	η_z (%)
Blank	110	125.2	0.969	187.79	
0.3	284	94.6	0.937	169.83	61.27
0.6	342	78.3	0.951	138.98	67.84
0.9	821	72.4	0.944	132.4	86.60
1.2	1260	58.8	0.956	98.52	91.27

3.3. FTIR Analysis

The FTIR spectrum of DPF extract is recorded in Figure 11. From the literature review it is clear that extracted DPF molecule containing major composition of hydroxyl and carbonyl groups are confirmed by IR bands.

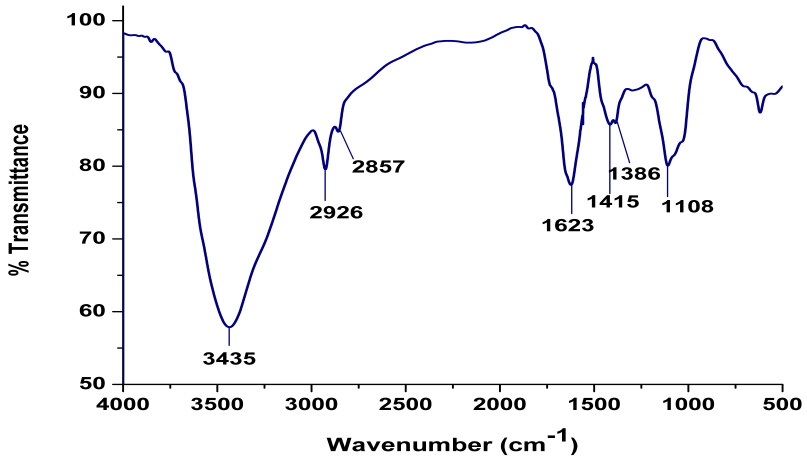

Figure 11: FTIR spectrum of DPF extract

The presence monomeric hydroxyl group (-OH) observed as strong, broad band at 3435 cm^{-1} and a sharp band observed at 1623 cm^{-1} indicates conjugated carbonyl (C=O) group. The aromatic and aliphatic CH stretching vibration is noticed at 2926 and 2857 cm^{-1} respectively and CH bending at 1415 and 1386 cm^{-1}. The phenolic C-O stretching is showed at 1108 cm^{-1}.

3.4. Surface Morphology Studies

Figure 12A and 12B represents SEM images of surface of the metal when dipped in 0.5M HCl and dipped in 1.2 g/L concentration of the DPF extract respectively. Comparison of the images with one another indicates that metal surface is more cracked in pure acidic media and these cracks are smoothened in the presence of inhibitor. The surface morphology studies agree the DPF extract behaves as inhibitor for protecting the mild steel from corrosion.

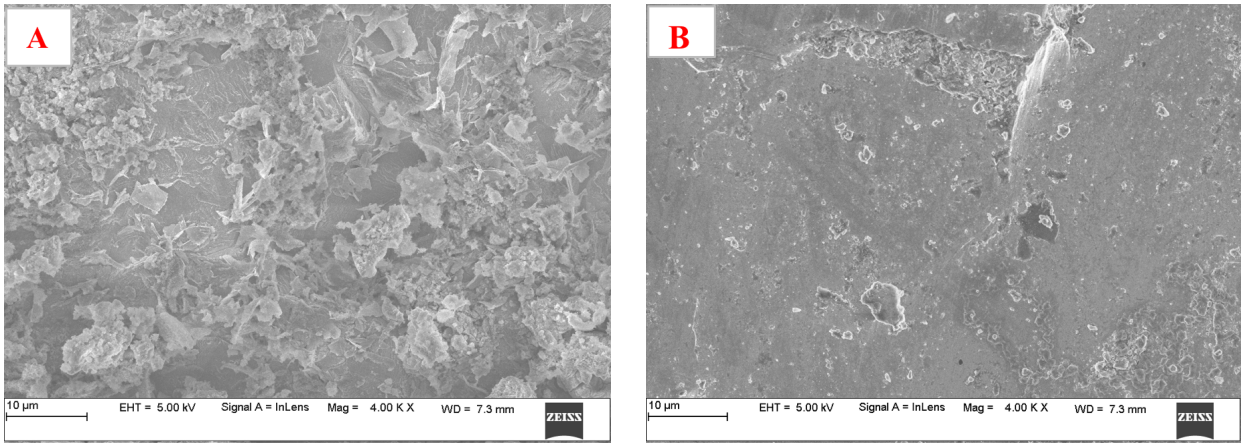

Figure 12: SEM images of Mild steel surface A) without inhibitor and B) with inhibitor respectively

Conclusion

The extraction of *Dillenia pentagyna* fruit in aqueous media using microwave irradiation was the easiest and fastest method and obtained good yield. The aqueous extract DPF is used as green corrosion inhibitor in acid media over the mild steel surface. The mass loss method clarified that rate of corrosion decreases as green inhibitor concentration increases with varying temperature. The protection efficiency of the DPF extract increases as its concentration increases. The protection process by both physisorption and chemisorptions in acid media obeys Langmuir adsorption isotherm. The behavior of mixed mode of the inhibitor through anodic and cathodic reaction is explained based on the electrochemical polarization studies. The protection of mild steel by adsorption was justified by AC impedance spectroscopic studies and modified the metal-electrolyte interface. The comparable results are obtained from gravimetric and electrochemical studies. These results are justified by images of the metal surface analysis by SEM.

Acknowledgements-The authors are grateful to Dr. A.V. Baliga College, Kumta for providing CH instrument for electrochemical studies.

References

1. H. Kumar, V. Yadav, *American Journal of Materials Science and Engineering,* 1(3) (2013) 34-39.
2. M. N. Desai, V. K. Shah, *Corros. Sci.* 12 (1972) 725-730.
3. E. Protopopoff, P. Marcus, Electrochemistry and materials science of cathodic hydrogen absorption and adsorption, PV 94-21. Conway, BE, Jerkiewicz, G, J. Electrochem Soc NJ 374-386 (1995).
4. G. Jerkiewicz, J. J. Borodzinski, W. Chrzanowski, B. E. Conway, *J. Electrochem. Soc.* 142 (1995) 3755-3763.
5. G. Rosangkima, S. B. Prasad, *Indian J. Exp. Biol.* 42 (2004) 981-988.
6. M. F. Haque, M. N. Islam, M. Hossain, A. U. Mohamad , M. F. Karim , M. A. Rahman, *Dhaka Univ. J. Pharm. Sci.* 7(1) (2008) 103-110.
7. R. K. Yadav, A. Prakash, *Med. Aromat. Plants,* 3 (2014) 160.

8. S. B. Prasad, G. Rosangkima, T. Rongpi, *Journal of Pharmacy Research,* 2(2) (2009) 243-249.
9. S. K. Srivastava, S. D. Srivastava, *Curr. Sci.* 53 (1984) 646-647.
10. A. Khanum, I. Khan, A. Ali, Ethnomedicine and Human Welfare, Ukaaz Publications (2007).
11. C. P. Khare, Indian Medicinal Plants New York: Springer (2007).
12. G. Ji, S. K. Shukla, P. Dwivedi, S. Sundaram, R. Prakash, *Ind. Eng. Chem. Res.* 50 (2011) 11954-11959.
13. O. Ghasemi, I. Danaee, G. R. Rashed, M. RashvandAvei, M. H. Maddahy, *J. Cent. South Univ.* 20 (2013) 301-311.
14. A. Ostovari, S.M. Hoseinieh, M. Peikari, S.R. Shadizadeh, S J. Hashemi, *Corros. Sci.* 51 (2009) 1935-1949.
15. M. Elachouri, M.S. Hajji, M. Salem, S. Kertit, J. Aride, R. Coudert, E. Essassi, *Corrosion,* 52 (1996) 103-108
16. S. Kumar, D. Sharma, P. Yadav, M. Yadav, *Ind. Eng. Chem. Res.* 52 (2013) 14019-14029.
17. E. A. Noor, *J. Appl. Electrochem.* 39 (2009) 1465–1475.
18. W. H. Li, Q. He, S. T. Zhang, C. L. Pei, B. R. Hou, *J. Appl. Electrochem.* 38 (2008) 289-295.
19. E. Bensajjay, S. Alehyen, M. El Achouri, S. Kertit, *Anti-Corros. Meth. Mater.* 50(6) (2003) 402-409.
20. X. Li, S. Deng, H. Fu, *Corros. Sci.* 51 (2009) 1344-1355.
21. M. Stern, A. L. Geary, *J. Electrochem. Soc*. 104 (1957) 56-63.
22. Z. Tao, S. Zhang, W. Li, B. Hou, *Ind. Eng. Chem. Res.* 50 (2011) 6082-6088.
23. M. K. Pavithra, T. V. Venkatesha, M. K. Punith Kumar, H. C. Tondan, *Corros. Sci.* 60 (2012) 104-111.

(2019) ; http://www.jmaterenvironsci.com/